ASSESSMENT OF THE CORRELATIONS BETWEEN AEROSOL OPTICAL DEPTH AND AIR TEMPERATURE

Neki FRASHERI
Academy of Sciences of Albania
Edmond LUKAJ
University of Shkodra, Faculty of Natural Sciences, Albania
Floran VILA
Academy of Sciences of Albania; University of Tirana, Faculty of Sciences, Albania
Florian MANDIJA
University of Shkodra, Faculty of Natural Sciences, Albania; French National Centre for Scientific Research (CNRS), Institute Pierre Simon Laplace (IPSL), Paris, France

---

ABSTRACT

Aerosols play a pivotal role in Earth's climate system, and their influence on temperature and other meteorological parameters remains a subject of active research. Aerosol Optical Depth (AOD) is closely associated with meteorological factors such as temperature and humidity because these variables can impact the concentration of aerosols in the atmosphere. The relationship between AOD and temperature is intricate, contingent on the specific attributes of the aerosols present in the atmosphere and the prevailing meteorological conditions. Some studies have reported a positive correlation between AOD and temperature, while others have found negative correlations or no discernible pattern. Aerosols can scatter and absorb sunlight, leading to either cooling or heating effects on the Earth's surface. This effect can be particularly pronounced in regions with high aerosol concentrations, such as urban areas or areas with elevated pollution levels. This study utilizes data from the MERRA-2 dataset, a comprehensive compilation of atmospheric and weather data acquired through satellite and other observing platforms. The analysis focuses on the territory of Albania, situated in Southeast Europe. The average correlation coefficient across the entire region is a statistically significant 0.56, with higher values observed in interior regions. A correlation coefficient ranging from 0.6 to 0.7 between AOD of black carbon and air temperature suggests a strong positive relationship between these two variables. Conversely, the relatively low correlation coefficients observed for other aerosol components such as organic carbon, sulfates, sea salt, and mineral dust with air temperature (Tair) imply weaker associations. Notably, the correlation coefficient for sea salt exhibits both positive and negative values.
***Keywords*:** aerosols, atmospheric parameters, correlation

1. INTRODUCTION

Climatic changes during the industrial age, starting from 1750, have had far-reaching consequences in various aspects of meteorology, notably the increase in global temperatures. Human-induced warming had reached approximately 1°C (likely between 0.8°C and 1.2°C) above pre-industrial levels by 2017, with an increase of 0.2°C (likely between 0.1°C and 0.3°C) per decade (high confidence) (IPCC, 2018). Global warming, its influencing factors, environmental effects, and future projections (Kaskaoutis *et al*., 2007) are central themes of 21st-century research (Figure 1). Within this realm of study, ongoing research focuses on climate change and its environmental repercussions, with over 2,000 articles published annually.

The Intergovernmental Panel on Climate Change (IPCC) is the foremost international organization dedicated to assessing climate change. The IPCC was established in 1988 by the United Nations Environment Programme (UNEP) and the World Meteorological Organization (WMO) with the mission of providing the world with a comprehensive scientific understanding of the current state of knowledge regarding climate change and its potential environmental and socio-economic consequences. The most recent IPCC Assessment Report (AR5) unequivocally affirms that human influence on the climate system is both evident and escalating, with observable impacts on every continent and ocean. Many of the changes observed since the 1950s are unprecedented over timescales spanning decades to millennia. The IPCC, with a 95% level of confidence, estimates that human activities are the primary driver of the ongoing global warming (IPCC 2013).

Fig. 1: The reciprocal effects of global warming and air pollution: greenhouse effect, drought due to high temperatures, extreme weather events, forest burning, melting of glaciers.

The primary human impact on the Earth's radiation budget is the emission of "greenhouse gases," with carbon dioxide being the most prominent among them. However, climate change manifests differently in various regions. Models and satellite observations have revealed that aerosols exert a net cooling effect on the climate, partially offsetting the global warming caused by greenhouse gases (Shindell *et al.,* 2012). Consequently, climate change has led to both the suppression and intensification of meteorological extremes like heatwaves, droughts, often accompanied by poor air quality conditions (García-Herrera 2010; *Trigo et al*., 2013). Aerosol emissions are significantly influenced by meteorological variables such as temperature, wind patterns, precipitation, among others, which in turn dictate the rate of their release into the atmosphere. Systematic assessments of aerosol particles and meteorological conditions have been conducted within the region (Mandija *et al*., 2016a and b; 2017- 2019). It's important to note that assessing the impact of climate change on air quality poses a considerable challenge due to the multifaceted nature of air quality, which depends on the interaction of multiple variables (Jimenez-Guerrero *et al*., 2013; Megaritis *et al*., 2014).

Regional assessments of these impacts are instrumental in reducing inaccuracies in global evaluations of climate-environmental interactions (Dentener *et al*., 2005).

The relationship between aerosol optical depth (AOD) and meteorological parameters has been a subject of study, but its underlying causes and radiative effects have remained unclear. Agreement regarding the dependence between AOD and air temperature is lacking. Some studies report a positive correlation between these parameters (Mamun, 2014; Li *et al*., 2021), while others suggest a negative correlation (Sen 2008). Conversely, some studies do not find a clear dependence (Mielonen 2016). Furthermore, certain studies have even shown an inverse relationship between the aerosol load in the atmosphere and the daily range of surface air temperature (Hu *et al*., 2021). Aerosols scatter and absorb sunlight during the daytime, thereby exerting a cooling or heating effect on the Earth's surface. This phenomenon plays a pivotal role in the context of climate change (Albrecht 1989; Hansen *et al*., 1995).

Among the primary optical and microphysical characteristics significantly influencing aerosols' role in climate modification are the Aerosol Optical Depth (AOD) and the Angstrom Exponent (AE) (O'Neill *et al*., 2007; Eck *et al*., 2001; Kaskaoutis *et al*., 2007). These parameters not only depend on local dynamics but also on the large-scale dynamics of the atmosphere. The relationship between AOD and temperature is complex and contingent upon the specific characteristics of aerosols present in the atmosphere and meteorological conditions (Mielonen *et al*., 2016).

This study examines the correlation between aerosol optical depth and air temperature (Tair) using data from MERRA-2, the most recent atmospheric reanalysis of the modern satellite era (Gelaro *et al*., 2017). The analysis focuses on the territory of Albania, situated in Southeastern Europe as part of the Western Balkans. Seasonal and spatial correlation coefficients, as well as the contribution of different aerosol types to this relationship, were determined for the 10-year period from 2005 to 2014.

2. METHODOLOGY

This study relies on NASA meteorological and atmospheric data, primarily utilizing the *Geospatial Interactive Online Visualization and Analysis Infrastructure* (GIOVANNI), a web-based application developed by the Goddard Earth Sciences Data and Information Services Center (GES DISC).

The primary aerosol optical parameters used for determining aerosol loads are the Aerosol Optical Depth (AOD) and Angstrom Exponent (AE), measured at 550nm and in the range of 470-870nm, respectively (Just *et al*., 2018). The dataset covers a 10-year period, from January 2005 to December 2014.

The spatial resolution of Aerosol Optical Depth (AOD) and air temperature (Tair) data provided by the Modern-Era Retrospective analysis for Research and Applications, Version 2 (MERRA-2) is 0.5° x 0.5°, covering the region within the coordinates: 19.50°E, 39.50°N, 20.75°E, 42.75°N, which entirely encompasses the territory of Albania. Temporally, daily, and monthly averaged data were processed, and further analyses were conducted on seasonal and yearly averaged data (Bali *et al*., 2017; Gelaro *et al*., 2017; Qin et al., 2019; Zhao *et al*., 2021).

Two types of data provided by GIOVANNI were utilized:

1. Spatial distribution data (in **nc** format), representing multiyear averages for each image pixel. These data were used to calculate correlation coefficients (CC) between aerosol and climate parameters. The images were previously converted into series of 3D coordinates (X, Y, Z), where X and Y denote the coordinates of the pixel center, and Z represents the parameter value.

2. Time series of daily/monthly data, averaged over specific areas and provided in csv format. These data were used to determine the correlation coefficients between different parameters within specific regions.

3. RESULTS AND DISCUSSIONS

Multi-annual seasonal averages of AOD and Tair

Table 1 reports the spatial correlations of 10-years averages of AOD and Tair over the Albanian territory, calculating their thematic values obtained in every pixel.

Tab. 1 Correlation coefficients between AOD and air temperature.

DJF (Dec-Jan-Feb)	MAM (Mar-Apr-May)	JJA (Jun-Jul-Aug)	SON (Sep-Oct-Nov)
0.12	0.24	0.46	0.59
Average Correlation (AC)	0.35	Global Correlation (GC)	0.66
Seasonal Correlation Average (SAC)	0.73	Average of Averages (AA)	0.77

The average correlation (AC=0.35) was calculated by averaging the thematic seasonal correlation coefficients between Tair and AOD across the entire Albanian territory for each season.

The Global Correlation (GC=0.65) is derived from the thematic seasonal averages of these quantities across the entire Albanian territory.

The thematic correlation coefficients between Tair and AOD were individually computed for each pixel during each season. Subsequently, the mean value of these correlation coefficients yielded the Seasonal Correlation Average (SAC=0.73±0.10).

Moreover, the Average of Averages (AA=0.77) represents the correlation coefficient between the seasonal mean values of Tair and AOD across all pixels.

As depicted in Table 1, the seasonal thematic correlation coefficients between Tair and AOD across pixels exhibit varying degrees of correlation. They range from 0.12 to 0.24 during DJF and MAM, increasing to 0.46 and 0.59 during JJA and SON, resulting in an overall average of AC=0.35±0.21. However, when seasonal distinctions are not considered, significantly higher values of the correlation coefficient are observed, such as GC=0.66. It's worth noting that the seasonal categorization of the data may contribute to the

overall reduction in the correlation coefficient. It should be mentioned that in both cases, the correlation analyses treat the pixels as the third variable.

Conversely, both Seasonal Correlation Average (SAC) and Average of Averages (AA) conduct correlation analyses across the four seasons. In this scenario, the correlation coefficients exceed 0.7. These findings indicate that the correlation coefficients are higher when the analysis is conducted separately for each pixel. Consequently, air temperature and aerosol optical depth exhibit a positive correlation for seasonal mean values at each pixel.

As depicted in Figure 2, the seasonal correlation coefficient (CC) exhibits a clearly defined unimodal curve (R2=0.73), a pattern also observed in monthly data (Li et al., 2021). The average of these data is 0.75, which closely aligns with their seasonal average (correlation average SAC=0.73). This observation underscores the exceptionally high correlation between the seasonal mean values of aerosol optical depth and air temperature. The scatter plot of these two variables, irrespective of the pixels, provides further evidence of their positive correlation, as illustrated in Figure 3.

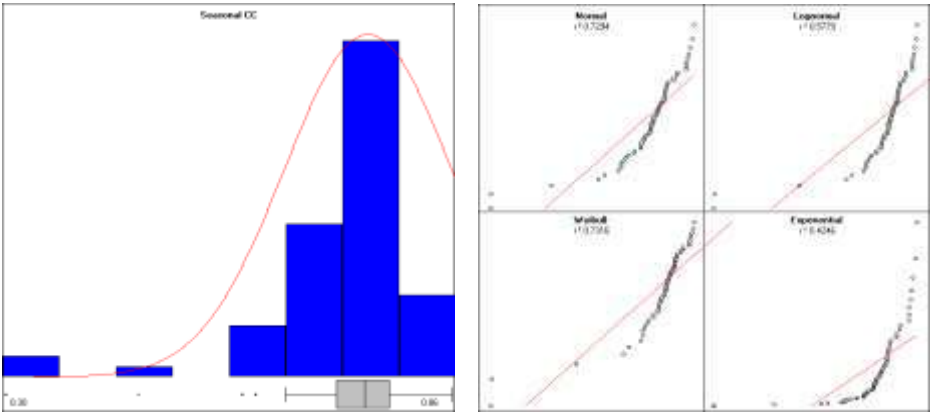

Fig. 2: Distributions of the Seasonal Correlation Coefficient (SAC) data.

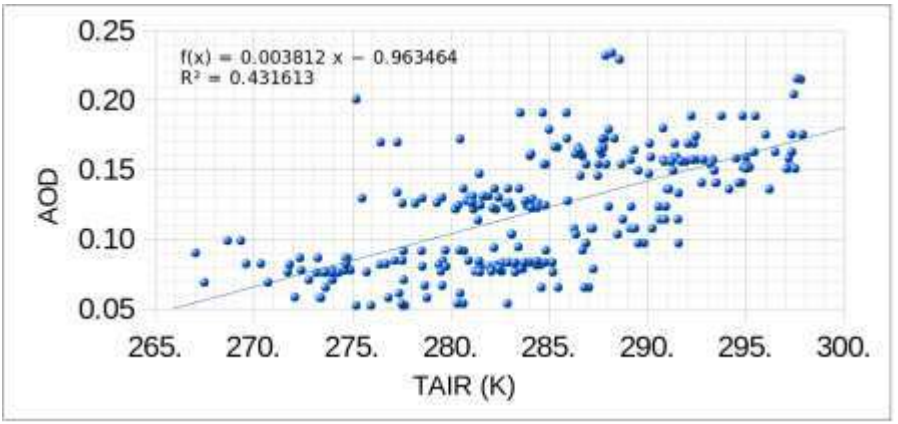

Fig. 3: Distribution of seasonal mean values of Tair and AOD over all pixels.

Although the distribution plot shows a positive relationship between seasonal mean values of AOD and Tair, the trend line has quite a slight slope (0.004) associated with relatively low R2=0.43. Thus, the scatterplot shows a weak positive relationship.

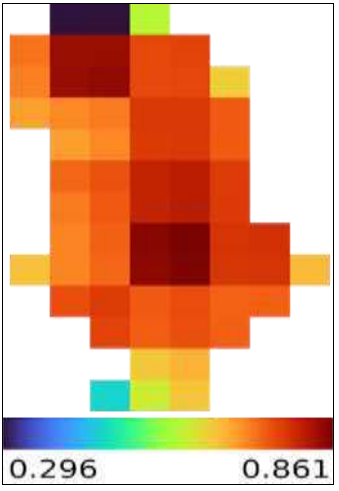

Fig. 4: Spatial distribution of correlation between the seasonal mean values of Tair and AOD in the Albanian territory

The map in the Figure 4 displaying the spatial distribution of the correlation coefficient (CC) reveals that Aerosol Optical Depth (AOD) is more closely linked to air temperature in the interior regions of the Albanian territory. The higher correlations observed in the interior can be attributed to the intensification of aerosol emission processes. This is primarily due to the

relatively limited industrial activities in this area, making anthropogenic emissions a secondary factor. Meanwhile, correlations in the western region, characterized by denser traffic, are weaker in comparison to the rest of the territory. Here, traffic emissions are less temperature-dependent, leading to weaker correlations. Additionally, Table 2 presents another perspective on this estimation, providing the annual mean values of the CC between the season averaged Tair and AOD.

Table 2 Annual-averaged of season correlation coefficients for the 10-years period; 2005-2014.

2005	2006	2007	2008	2009	2010	2011	2012	2013	2014
0.89	0.57	0.94	0.73	0.10	0.19	0.79	0.63	0.23	0.53
Average		0.56	Global		0.50				

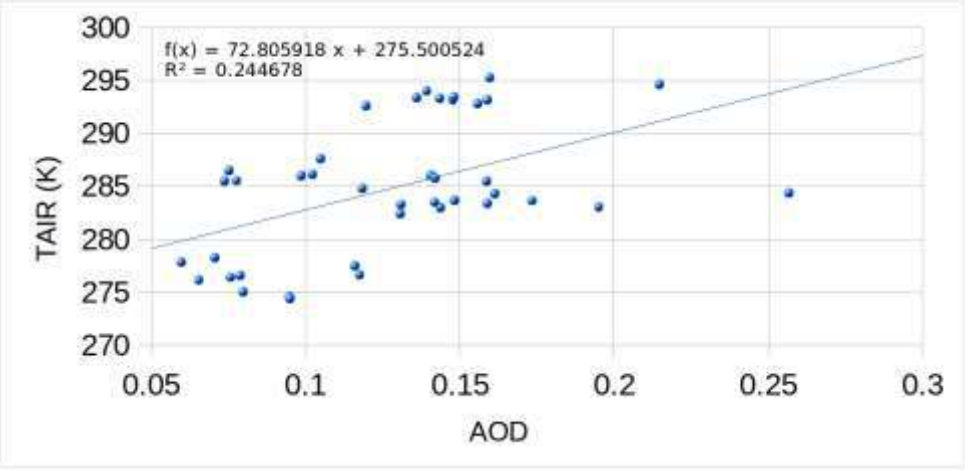

Fig. 5: Distribution of annual mean AOD and Tair values over all pixels

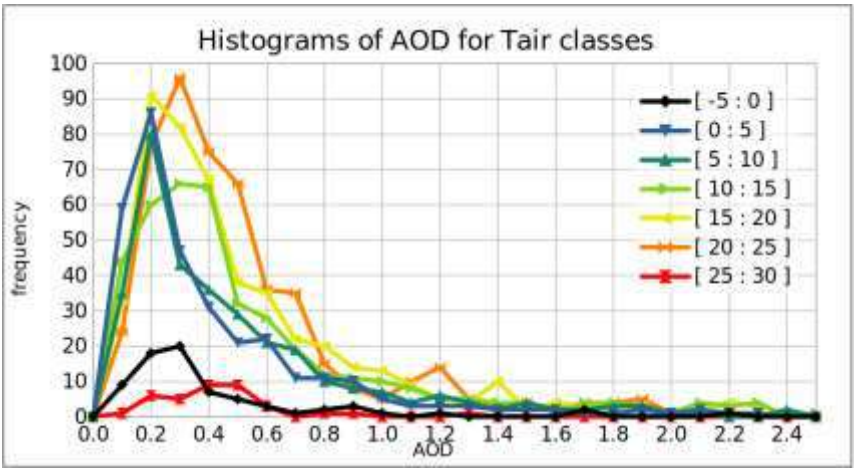

Fig. 6: Histograms of the daily-averaged data of the AOD frequency distributions for seven Tair classes of 5 degrees. Here, all the pixels have been considered.

Significant fluctuations in the correlation coefficient (CC) values are evident across different years. Very weak correlations (CC=0.1 and 0.19) were observed during 2009-2010, while strong correlations were observed in 2005 (CC=0.89) and 2007 (CC=0.94). However, the average and global CC values in this context are notable, with nearly identical magnitudes of 0.56 and 0.50, respectively. The distribution of these values in Figure 5 indicates a positive relationship between these two variables, although the R2 of the trend line is not notably high at 0.24.

To gain a more comprehensive understanding of the correlation between aerosol optical depth and air temperature, we conducted a distribution analysis of their daily-averaged values grouped into seven Tair classes. Figure 6 illustrates the seven histograms of AOD for different Tair classes.

The distribution of daily averaged AOD averages for all Tair classes reveals distinct characteristics. This observation is further detailed in Table 3, which presents the mean and median values of AOD for each Tair class.

Tab. 3 Features of the statistical distributions of the daily-averaged AOD for all Tair classes

	(-5:0)	(0:5)	(5:10)	(10:15)	(15:20)	(20:25)	(25:30)
Mean	0.37	0.38	0.45	0.50	0.49	0.48	0.38
Median	0.24	0.25	0.31	0.34	0.34	0.36	0.36
R^2 (lognormal)	0.98	0.99	0.99	0.99	0.99	0.99	0.97

The average AOD demonstrates an increase with rising air temperature, reaching a peak of 0.50 within the temperature range of 10-25°C, followed by a sharp decline to 0.38. Conversely, the average AOD exhibits a continuous increase with increasing air temperature, ranging from 0.24 to 0.36. These patterns align with the characteristics of lognormal distributions, which is also the case here. Figure 7 illustrates the statistical distributions of the daily-averaged AOD values.

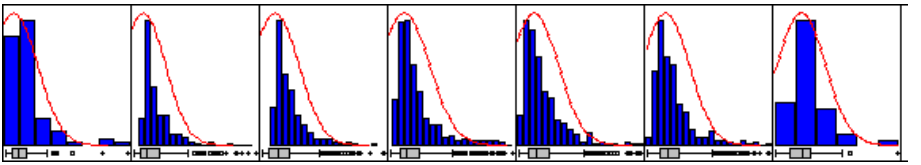

Fig. 7: Distribution of average AOD at seven different Tair classes.

Estimating the contributions of different types of aerosols

A more in-depth and nuanced understanding of the relationship between Aerosol Optical Depth (AOD) and air temperature (Tair) can be achieved when considering the various types of aerosols. To delve into this, we've examined the spatial distribution of contributions to AOD across the entire territory of Albania.

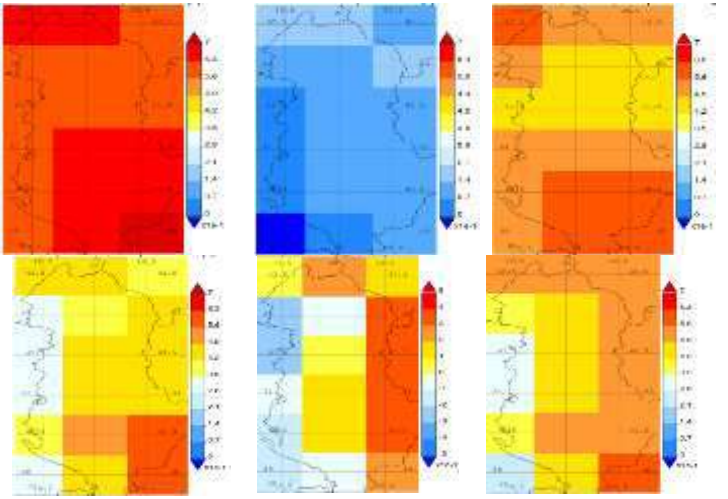

Fig. 8: Maps of the monthly-averaged values of the correlation coefficient between AOD and Tair for different aerosol types. From top-left to bottom-right; black carbon (BC), mineral dust, organic carbon (OC), sulphates (SO4), sea salt, and the total AOD.

Figure 8 displays the spatial distribution of monthly-averaged values of the correlation coefficient between AOD and Tair for various aerosol types, including dust, carbonaceous aerosols, sulfates, and the total aerosol contribution. The CC scale ranges from 0 to 0.7 for all types of aerosols, except for sea salt, where the CC varies within the range of -0.7 to 0.7.

From the maps above, it's evident that AODBC-Tair exhibits higher correlation coefficients (CC) across most of the territory (CC=0.6÷0.7), with even higher values observed in the southeastern regions. The strong correlation between AODBC and Tair can be attributed to the fact that black carbon (BC) particles are primarily generated during episodes of high temperatures. These episodes result from intensified sources, including biomass combustion, natural sources, and anthropogenic sources such as cooking and low-temperature heating, which prevent the complete combustion of compounds (Zha *et al*., 2014). Correlation analyses between BC and air temperature are influenced by wind speed, a significant factor in BC diffusion within the boundary atmosphere. Partial correlation coefficients may provide a more appropriate approach for investigation. The increase in BC is likely associated with fossil fuel combustion during the winter heating period, biomass burning in surrounding areas during the summer harvest period, and long-range transport. The positive correlation between AODBC and Tair suggests a more pronounced impact of biomass burning compared to warming. Conversely, relatively low CC values were obtained for other aerosol components, such as organic carbon (OC), sulfates, and sea salt, while the contribution of mineral dust to AOD does not appear strongly correlated with air temperature.

The CC of AOD_{dust}-Tair values remains insignificant across the entire territory (with a maximum CC of 0.2). This suggests that the presence of dust in the Albanian territory is primarily a result of long-range transport rather than local sources, which may be more active at higher temperature levels. The transport of dust from nearby deserts is typically determined by the flow of air masses rather than local temperature variations. Additionally, the CC of AODOC-Tair ranges from 0.4 to 0.6, with higher values observed in the southeastern region. However, it's worth noting that AODOC carries less weight compared to other aerosol components. Its maximum values are found in the northern part of the coastal region, while the southeastern region, with the highest CC, is less impacted by organic carbon aerosols. Despite the lower AODOC values, their mean values do follow the air temperature trend. They peak during the July-September period (AODOC=0.02÷0.05) and reach their minima during the cold November-February period (AODOC≈0.01).

Organic aerosols are emitted as primary aerosol organic carbon from fossil fuel burning or formed as secondary aerosol particles through the condensation of organic gases with semi-volatile or low volatility properties

(Zhang *et al*., 2016). These sources do not follow the same annual cycle, which contributes to the relatively low CC values in this case and suggests a limited contribution of organic carbon (OC) aerosols to AOD. Notably, atmospheric concentrations of organic aerosol are often comparable to those of industrial sulfate aerosol. As a result, the CC of AODSO4-Tair exhibits higher values in the southeastern region and lower values along the sea coast, though these differences are not highly significant (ranging from 0.3 to 0.6). AODSO4 somewhat mirrors the annual cycle of Tair, with the highest presence of sulfate aerosols occurring during the warm months of April-September (AODSO4=0.10÷0.13) and the lowest contribution during the cold period of November-January (AODSO4=0.05÷0.08). This observation aligns well with previous studies, which indicate that the majority of regional atmospheric sulfate aerosol accumulation episodes typically occur in the warmer months of the year. However, in the interior regions, AODSO4 better follows the annual cycle of Tair, resulting in higher AODSO4-Tair values over these areas. The interior regions are affected not only by long-range transport but also by local contributions, as sulfate aerosols in the atmosphere are associated with the combustion of fossil fuels (Kleindienst *et al*., 2010).

In addition, the correlation between AODsalt and Tair is negative over the western seashore region (-0.3÷-0.1) and positive in the eastern region (0.2÷0.4). CC AODsalt-Tair remains intermediate over the inner regions. Thus, the spatial distribution of the sea salt correlation with the air temperature exerts a specific pattern due to the proximity to the Adriatic Sea. It must be mentioned that the highest sea salt presence occurs during the cold period due to the intensive wind activity. That is the reason for the negative correlation between sea salt presence and the air temperature. Meanwhile, positive correlations were obtained over remote areas from the sea, where the salt contribution on AOD is negligible. The regression analysis shown in Figure 9 provides more insights into the correlation of different AOD components with the air temperature.

For all the cases the trendline show positive correlations between AOD components and the air temperature. However, the slopes of the trendlines are quite different between the AOD components; BC (0.0002), dust (0.0006), OC (0.0009), sea salt (0.0002), SO4 (0.0017) and the total AOD (0.0037). The total AOD shows a good correlation with Tair, mainly due to the impact of the SO4 contribution. Other components show lesser correlations with the air temperature. This is more evident for the case of BC and sea salt, but also for the dust and even for OC component of AOD.

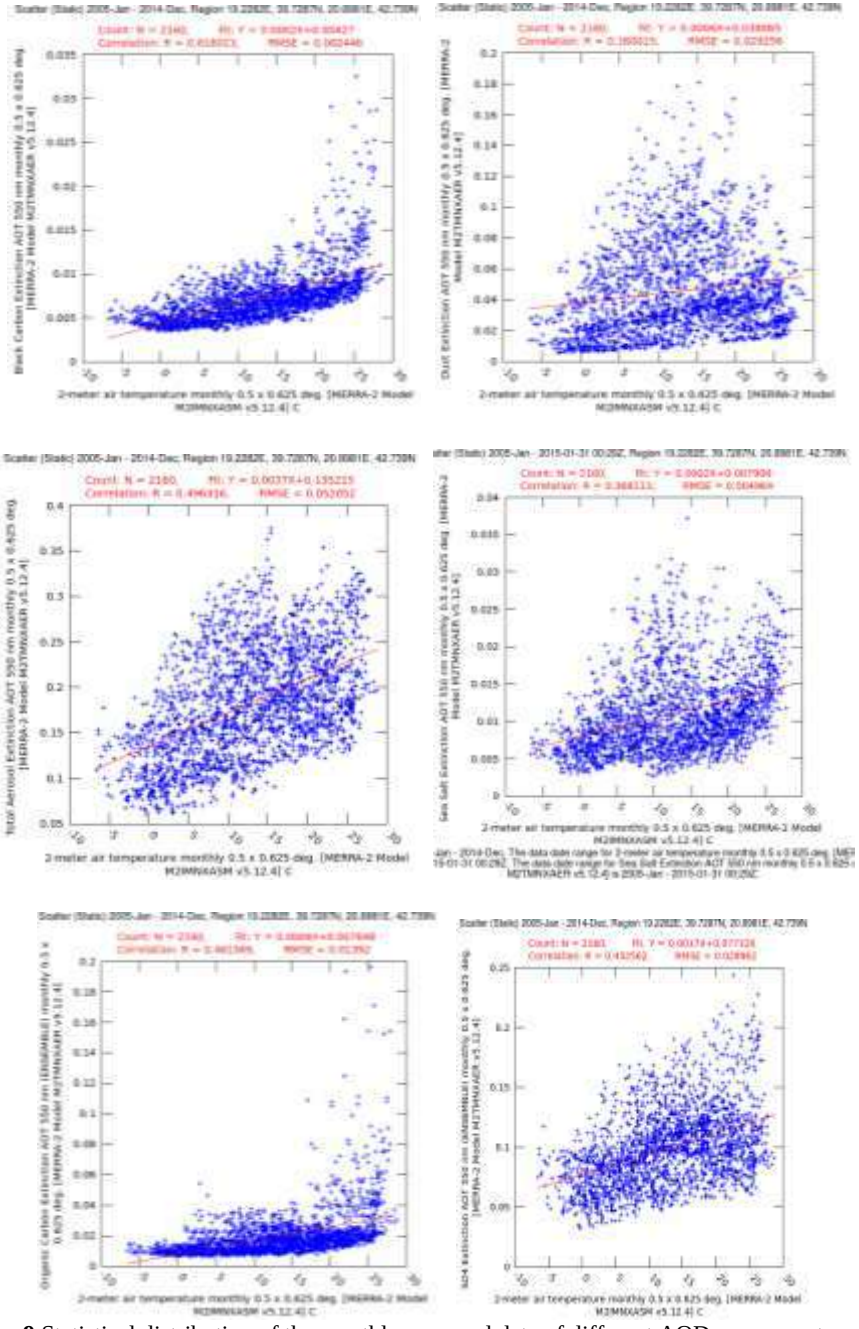

Fig. 9 Statistical distribution of the monthly averaged data of different AOD components and air temperature. Also, the linear trend line is included.

4. CONCLUDING REMARKS

In this paper, we conducted a correlation study between aerosol optical depth and air temperature using data provided by the Retrospective Analysis of the Modern Era for Research and Applications, Version 2 (MERRA-2), for the territory of Albania.

Seasonal correlation coefficients, which ranged from 0.12 to 0.59, indicate a significant correlation only during the period from June to November. However, correlation coefficients higher than 0.70 were achieved when the analysis was performed for each pixel separately. This is evident in the seasonal correlation data representing the Seasonal Correlation Average (SCA) of 0.73. Additionally, the scatterplot demonstrates a positive correlation between the seasonal mean values of AOD and Tair, with a trendline slope of approximately 0.004.

When examining the correlation map, the highest correlations are evident in the interior regions of the territory, where natural aerosol emission processes are more pronounced. We observed a significant variation in annual mean values of the correlation coefficients. The average correlation coefficient in this case stands at 0.56.

When estimating the AOD data across different Tair (air temperature) classes, we noticed distinct statistical differences between mean and median AOD values. The mean AOD reaches its peak at 0.50 in the temperature interval of 10-25°C, while the median AOD steadily increases with rising air temperatures, reaching its maximum value of 0.36.

It's worth noting that various aerosol types have distinct effects on meteorological parameters through their interactions with sunlight. However, this study primarily focuses on examining the variation in their contribution to AOD and air temperature without considering their radiative effects.

Correlation coefficients between different AOD components and Tair reveal that AODBC-Tair exhibits higher correlation coefficients, ranging from 0.6 to 0.7, across most of the territory, with even higher values in the southeastern regions. These regions experience more intense biomass burning processes during the warm seasons, with anthropogenic sources playing a secondary role. In contrast, other aerosol components like OC, sulphates, and sea salt show relatively lower correlation coefficients, around 0.3 to 0.6. Interestingly, the contribution of mineral dust to AOD doesn't appear to be strongly correlated with air temperature (CC=0.2). This lower correlation can be attributed to the significant influence of long-range transport compared to local dust emissions. The various organic aerosol sources exhibit distinct annual cycles, making them less responsive to air temperature variations. Atmospheric concentrations of organic aerosols often resemble those of

industrial sulphate aerosols, with the highest sulphate aerosol AOD occurring during warm periods.

Furthermore, the correlation between AODsalt and Tair varies across different regions, ranging from -0.3 to -0.1. Notably, the highest AODsalt levels are observed during the cold period due to intense wind activity. This explains the negative correlation between sea salt presence and air temperature, especially along the seashore regions. Additionally, scatterplot trendlines display positive correlations between AOD components and air temperature, accompanied by slight trendline slopes for the AOD components, including BC, sea salt, dust, OC (0.0002 to 0.0006), and SO4 (0.0017), while the slope for the total AOD is 0.0037.

ACKNOWLEDGMENTS

The authors would like to express their gratitude to the Albanian National Agency for Scientific Research and Innovation (NASRI) for their financial support in the realization of the project titled, *Assessment of the reciprocal impacts between climate change and air pollution on the territory of Albania*. This paper constitutes an integral part of that project. We would also like to extend our appreciation to the US NASA-MODIS for providing the data used in this study, as well as to the US NOAA Air Resources Laboratory (ARL) for making the HYSPLIT model and NAAPs maps available, which were essential for our research. Furthermore, we are grateful to the READY website for its valuable resources used in this paper. Special thanks go to the NASA-MODIS aerosol team for providing the data from MODIS-TERRA. We would also like to acknowledge the Giovanni team at the NASA GES DISC (Goddard Earth Sciences Data and Information Services Center) for their continuous efforts in maintaining and providing access to the Giovanni data analysis system for NASA's research community.

REFERENCES

Albrecht BA. 1989. Aerosols, Cloud Microphysics, and Fractional Cloudiness. *Science*, **245 (4923):** 1227–1230 CrossRef CAS. DOI: 10.1126/science.245.4923.1227.

Bali K, Mishra AK, Singh S. 2017. Impact of anomalous forest fire on aerosol radiative forcing and snow cover over Himalayan region. *Atmospheric Environment*, **150**: 264–275. doi:10.1016/j.atmosenv.2016.11.061.

Dentener F, Stevenson D, Cofala J, Mechler R, Amann M, Bergamaschi P, Raes F, Derwent R. 2005. The impact of air pollutant and methane emissions controls on tropospheric ozone and radiative forcing: CTM calculations for the period 1990–2030. *Atmospheric Chemistry and Physics*, **5:**1731–1755. https://doi.org/10.5194/acp-5-1731-2005.

Eck TF, Holben BN, Dubovic O, Smirnov A, Slutsker I, Lobert JM, Ramanathan V. 2001. Column-integrated aerosol optical properties over the Maldives during the northeast monsoon for 1998–2000. *Journal of Geophysical Research*, **106 (D22):** 28.555–28. 566.

García-Herrera R, Díaz J, Trigo RM, Luterbacher J, Ficher E. 2010. A review of the European summer heat wave of 2003. *Critical Reviews in Environmental Science and Technology*, **40**: 267 – 306.

Gelaro R, McCarty W, Suárez MJ, Todling R, Molod A, Takacs L, Randles CA, Darmenov AS, Bosilovich MG, Reichle RH, Wargan K, Coy L, Cullather RI, Draper C, Akella S, Buchard V, Conaty A, Silva AM, Gu W, Kim G, Koster RD, Lucchesi R, Merkova D, Nielsen JE, Partyka, G., Pawson S, Putman WM, Rienecker MM, Schubert S, Sienkiewicz M, Zhao B. 2017. The Modern-Era Retrospective Analysis for Research and Applications, Version 2 (MERRA-2). *Journal of climate*, **30(13)**: 5419-5454.

Hansen J, Sato M, Ruedy R. 1995. Long-term changes of the diurnal temperature cycle: implications about mechanisms of global climate change. *Atmospheric Research*, **37**: 175–209.

Hu S, Wang D, Wu J, Zhou L, Fu T, Yang X, Ziegler A, Zeng Z. 2021. Aerosol presence reduces the diurnal temperature range: an interval when the COVID-19 pandemic reduced aerosols revealing the effect on climate. *Environmental Science: Atmospheres*, **1:** 208-213. The Royal Society of Chemistry. https://doi.org/10.1039/D1EA00021G.

IPCC, Allen MR, Dube OP, Solecki W, Aragón-Durand F, Cramer W, Humphreys S, Kainuma M, Kala J, Mahowald N, Mulugetta Y, Perez R, Wairiu M, Zickfeld K. 2018. Framing and Context. In: Global Warming of 1.5°C. An IPCC Special Report on the impacts of global warming of 1.5°C above pre-industrial levels and related global greenhouse gas emission pathways, in the context of strengthening the global response to the threat of climate change, sustainable development, and efforts to eradicate poverty.

Jiménez-Guerrero P, Jerez S, Montávez JP, Trigo RM. 2013. Uncertainties in future ozone and PM10 projections over Europe from a regional climate Multiphysics ensemble, *Geophysical Research Letters*, **40(21) :** 5764-5769. doi:10.1002/2013GL057403.

Just AC, De Carli MM, Shtein A, Dorman M, Lyapustin A, Kloog I. 2018. Correcting Measurement Error in Satellite Aerosol Optical Depth with Machine Learning for Modeling PM2.5 in the Northeastern USA. *Aerosol Remote Sensing*, **10:** 803. https://doi.org/10.3390/rs10050803.

Kaskaoutis DG, Kosmopoulos PG, Badarinath KVS. 2007. Aerosol climatology: dependence of the Angstrom exponent on wavelength over four AERONET sites. *Atmospheric Chemistry and Physics*, 7347-7397. https://doi.org/10.5194/acpd-7-7347-2007.

Kleindienst TE, Lewandowski M, Offenberg JH, Edney EO, Jaoui M, Zheng M, Ding X, Edgerton ES. 2010. Contribution of primary and secondary sources to organic aerosol and PM2.5 at SEARCH network sites. *Journal of the Air & Waste Management Association (1995)*, 60 **(11):** 1388-99. doi:10.3155/1047-3289.60.11.1388.

Li J, Ge X, He Q, Abbas A. 2021. Aerosol optical depth (AOD): spatial and temporal variations and association with meteorological covariates in Taklimakan desert, China. *PeerJ*, **5;9:e10542**. doi: 10.7717/peerj.10542. PMID: 33505790; PMCID: PMC7792517.

Mamun MM. I. 2014. An observational study of aerosol optical properties and their relationships with meteorological parameters over Bangladesh. *IOSR Journal of Applied Geology and Geophysics*, **2(6):** 75–84. https://doi.org/10.9790/0990-02617584.

Mandija, F. J. L. Guerrero-Rascado, H. Lyamani, M. J. Granados-Muñoz, L. Alados-Arboledas. 2016a. Synergic estimation of columnar integrated aerosol properties and their vertical resolved profiles in respect to the scenarios of dust intrusions over Granada. *Atmospheric Environment*, **145**: 439-454.

Mandija F, Markowicz K, Zawadzka O. 2016b. Characterization of aerosol events using synergistically column integrated optical aerosol properties and polarimetric measurements. *Journal of Atmospheric and Solar-Terrestrial Physic*s. **150:** 9-20.

Mandija F, Sicard M, Comerón A, Alados-Arboledas L, Guerrero-Rascado JL, Barragán R, Bravo-Aranda JA, Granados-Muñoz MJ, Lyamani H, Muñoz Porcar C, Rocadenbosch F, Rodríguez A, Valenzuela A, García Vizcaíno D. 2017. Origin and pathways of the mineral dust transport to two Spanish EARLINET sites: Effect on the observed columnar and range-resolved dust optical properties. *Atmospheric Research*, **187**; 69-83.

Mandija F, Chavez Perez VM, Nieto R, Sicard M, Danylevsky V, Anel J-A, Gimeno L. 2018. The climatology of dust events over the European continent using data of the BSC-DREAM8b model. *Atmospheric Research*, **209**: 144-162.

Mandija F, Vila F, Lukaj E, Bushati J. 2019. Desert dust episodes over Balkan Peninsula. Proceedings of the 10th Balkan Physical Union. *American Institute of Physics*, **2075 (1):** 130011; https://doi.org/10.1063/1.5091296.

Megaritis AG, Murphy BN, Racherla PN, Adams PJ, Pandis SN. 2014. Impact of climate change on mercury concentrations and deposition in the eastern United States. Sci. Total Environ., 487, 299-312, doi:10.1016/j.scitotenv.2014.03.084.

Mielonen T, Hienola A, Kühn T, Merikanto J, Lipponen A, Bergman T, Korhonen H, Kolmonen P, Sogacheva L, Ghent D, Arola A, de Leeuw G, Kokkola H. 2016. Temperature-dependence of aerosol optical depth over the southeastern US, Atmos. *Atmospheric Chemistry and Physics*, [preprint], https://doi.org/10.5194/acp-2016-625.

O'Neill NT, Dubovic O, Eck TF. 2001. Modified Angström exponent for the characterization of submicrometer aerosols. *Applied optics*, 40 (15): 2368-75. doi:10.1364/ao.40.002368.

Qin W, Zhang Y, Chen J, Yu Q, Cheng S, Li W, Liu X, Tian H. 2019. Variation, sources, and historical trend of black carbon in Beijing, China based on ground observation and MERRA-2 reanalysis data. *Environmental pollution (Barking, Essex: 1987)*, **245**: 853-863. doi:10.1016/j.envpol.2018.11.063.

Sen S. Roy 2008. Impact of aerosol optical depth on seasonal temperatures in India: a spatio-temporal analysis, *International Journal of Remote Sensing*, **29(3):** 727-740, DOI: 10.1080/01431160701352121.

Shindell D, Lamarque J-F, Schulz M, Flanner M, Jiao C, Chin M, Young PJ, Lee YH, Rotstayn L, Mahowald N, Milly G, Faluvegi G, Balkanski Y, Collins WJ, Conley AJ, Dalsoren S, Easter R, Ghan S, Horowitz L, Liu X, Myhre G, Nagashima T, Naik V, Rumbold ST, Skeie R, Sudo K, Szopa S, Takemura T, Voulgarakis A, Yoon J-H, Lo. 2013. Radiative forcing in the ACCMIP historical and future climate simulations. *Atmospheric Chemistry and Physics*, **13(6):** 2939–2974.

Trigo RM, Añel J, Barriopedro D, García-Herrera R, Gimeno L, Nieto R, Castillo R, Allen MR, Massey N. 2013. The record Winter drought of 2011-12 in the Iberian Peninsula, in Explaining Extreme Events of 2012 from a Climate Perspective. *Bulletin of the American Meteorological Society*, **94 (9):** S41-S45.

Zha S, Chenga T, Tao J, Zhange R, Chena J, Zhang Y, Leng C, Zhang D, Du J. 2014. Characteristics and relevant remote sources of black carbon aerosol in Shanghai. *Atmospheric Research,* **135-136:**159-171.

Zhang YL, Kawamura K, Agrios K, Lee M, Salazar G, Szidat S. 2016. Fossil and Nonfossil Sources of Organic and Elemental Carbon Aerosols in the Outflow from Northeast China. *Environmental Science and Technology,* **50(12):**6284-92. doi: 10.1021/acs.est.6b00351. PMID: 27203471.

Zhao J, Liu Y, Shan M, Liang S, Cui C, Chen L, Gao S, Mao J, Zhang H, Sun Y, Ma Z, Yu S. 2021. Characteristics, potential regional sources, and health risk of black carbon based on ground observation and MERRA-2 reanalysis data in a coastal city, China. *Atmospheric Research* **256**: 105563. doi:10.1016/j.atmosres.2021.105563.